ELSEVIER

Polymer 41 (2000) 2569–2576

polymer

Structure development in multi-block copolymerisation: comparison of experiments with cell dynamics simulations

I.W. Hamley[a,1], J.L. Stanford[b], A.N. Wilkinson[c], M.J. Elwell[d], A.J. Ryan[e,*]

[a]*School of Chemistry, University of Leeds, Leeds LS2 9JT, UK*
[b]*Materials Science Centre, UMIST, Manchester M1 7HS, UK*
[c]*Department of Chemistry and Materials, Manchester Metropolitan University, Manchester M1 5GD, UK*
[d]*Polyglycols Innovation Centre, Dow Benelux N.V., Herbert H. Dow weg, Post box 48, 4530 AA Terneuzen, The Netherlands*
[e]*Department of Chemistry, University of Sheffield, Dainton Building, Sheffield S3 7HF, UK*

Received 1 January 1999; received in revised form 22 April 1999; accepted 25 May 1999

Abstract

A cell dynamics simulation of phase separation in block copolymers is compared with experimental observations for two related systems, polyurethane (poly(ether-urea)) foam and poly(ether-isocyanurate). Time resolved SAXS measurements on both systems suggest a spinodal-like mechanism with kinetics following a time-dependent Ginzburg–Landau (TDGL) model. TEM micrographs from a range of sources show reactively processed multi-block copolymers to have a bicontinuous morphology, which is discussed as a non-equilibrium relic of the phase separation process. A TGDL based cell-dynamics model gives predictions of the morphology, which can be compared to TEM images and SAXS patterns. The model does not contain any reactive aspects but captures the morphology of the systems which both showed pinning of the micro-structure at early stages of microphase separation in contrast to the equilibrium structures formed by block copolymers.

Keywords: Polyurethane; Ginzburg–Landau model; Bicontinuous morphology

1. Introduction

Block copolymers are an important class of materials due to their ability to self-assemble and the resulting unique combinations of properties [1]. There are effectively two commercial routes to the synthesis of block copolymers. [2] Anionic polymerisation is used to make very well-characterised di-block and tri-block copolymers by sequential monomer addition to a living polymerisation and tends to form polymers with narrow molar mass distributions of both the blocks per chain and of the block length. Step polycondensation is used to make multi-block copolymers and industrially these are made via one-step bulk reactions where a low T_g oligomer is introduced into a polymerisation forming a high T_m polymer. A typical example is the use of a polyether polyol in the reaction between water and an aromatic isocyanate to form a segmented block co-poly(ether-urea) which has rubbery polyether segments and glassy (pseudo-crystalline) polyurea segments. Typically this process is used to make polyurethane foam via either the continuous slab-stock process or the reaction injection moulding (RIM) process [3]. Step copolycondensations form multi-block copolymers with statistical distributions in both the blocks per chain and in the block lengths.

The unique combination of physical properties provided by segmented block copolymers is related to their microphase-separated morphologies. The development of a microphase-separated morphology during polymerisation is complex. As the different chemical reactions proceed, chain lengths increase giving an increase in the overall degree of polymerisation, N. Additionally, the interaction parameter (χ), characterising the miscibilities between the different segments also increases as a result of polymerisation. In the specific case of segmented block copolymerisation, such changes in χ and N (or more strictly the product χN) drive the system across thermodynamic boundaries and result in a transition from an initial homogeneous (disordered) state to a microphase-separated (ordered) state. The resultant morphology is determined by the competition between the kinetics of polymerisation and microphase separation [4,5]. Further, homopolymeric and oligomeric species may undergo macrophase separation and the copolymer morphology that eventually evolves may reflect

* Corresponding author. Tel.: + 44-0114-222-9409; fax: + 44-0114-222-9303.
E-mail address: tony.ryan@sheffield.ac.uk (A.J. Ryan)
[1] Corresponding author.

0032-3861/00/$ - see front matter
PII: S0032-3861(99)00401-2

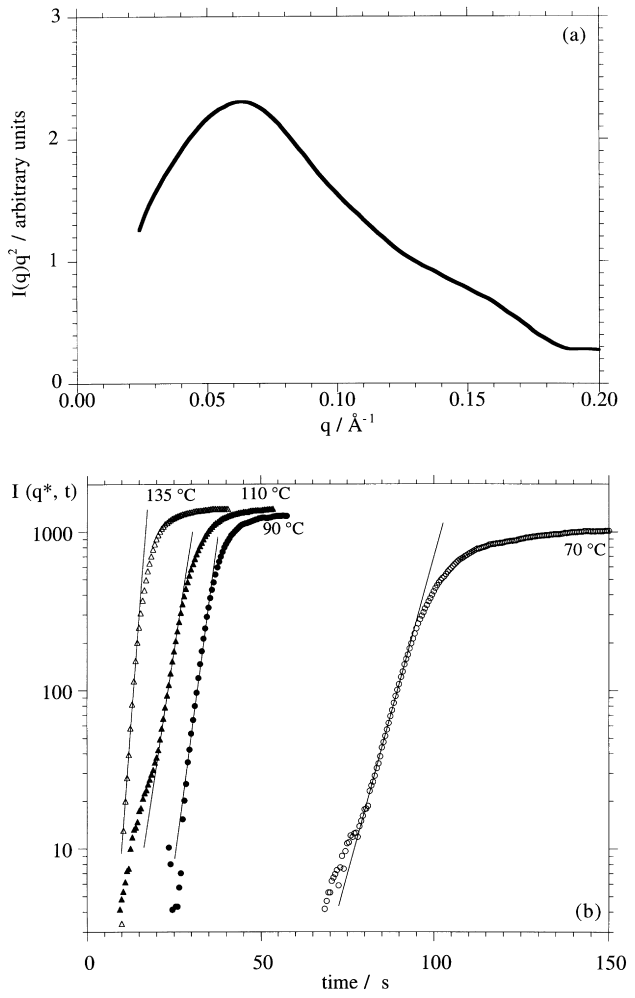

Fig. 1. (a) A SAXS patterns obtained during the polymerisation of a poly(ether-isocyanurate) with a volume fraction of polyether of 0.33. Lorentz-corrected intensity, $I(q)q^2$, versus scattering vector, q, 68 s after mixing at a cell temperature of 90°C. (b) Peak intensity, $I(q^*, t)$, versus time, t, for the cell temperatures 70, 90, 110 and 135°C [14].

phase separation and/or vitrification, crosslinking or crystallisation and is determined by the competition between the kinetics of these processes.

Understanding the complex competition between polymerisation and microphase separation requires in situ, time-resolved analytical techniques. In multi-phase systems, FTIR spectroscopy and rheometry are used to obtain chemical and macroscopic property information during polymer formation. Investigation of the kinetics of structure formation requires time-resolved scattering techniques such as SAXS and SALS, depending on the length scales of the evolving molecular structures [6]. Such in situ SAXS experiments during foam formation, employing a forced-adiabatic SAXS sampling cell positioned in the optical bench assembly of a synchrotron beam line, have been reported by Elwell et al. [7].

The kinetics of ordering in block copolymer melts has been studied using cell dynamical simulations (CDS) of the time-dependent Ginzburg–Landau (TDGL) equation [8–13]. In block copolymers, the order parameter represents the spatial variation of monomer density:

$$\langle \psi(\mathbf{r}) \rangle = \langle \rho_A(\mathbf{r}) - f \rangle \quad (1)$$

where $\rho_A(\mathbf{r})$ is the local density of monomer A and f is the average density. In the CDS method the continuous order parameter (Eq. (1)) is discretized on a lattice and at time t is denoted $\psi(t, n)$, where n labels the lattice site. Kinetic equations for the time-evolution were obtained by Puri and Oono [10]. They are governed by the underlying physical forces arising from the local driving force for phase separation due to the chemical potential and the diffusive effect due to the difference of the order parameter value in neighbouring cells. This method was first applied to block copolymer melts by Bahiana and Oono [8], who investigated the development of microphase-separated structures for asymmetric and symmetric block copolymers in two dimensions, starting from an initially disordered configuration. Although the effects of boundary conditions and hydrodynamics in obtaining highly oriented lamellae was also studied by Bahiana and Oono [8], Shiwa et al. [13] have recently investigated the kinetics of structure factor development for microphase separation of two-dimensional lamellae. Qi and Wang [11,12] have recently developed CDS simulations of the TDGL equation to consider the evolution of structure following a temperature jump from one phase to another. They considered temperature jumps between all classical ordered phases (lamellae, hexagonal and cubic) and the disordered phase [12]. The TDGL equations were simulated in three dimensions using the CDS method, and additionally mode analyses were performed in the single-wave number approximation, which reduces the problem to a series of coupled equations describing the steepest descent of the order parameters on the free energy surface. Analysis of the TDGL equation via CDS simulations is one of the most promising approaches to the study of dynamics in block copolymer melts.

The purpose of this paper is to compare experimental and simulation results for structure development during a copolymerisation reaction. We compare experimental observations of the kinetics of microphase separation during the reactive processing of multi-block copolymers and their final morphology with a cell dynamics simulation. The TDGL model is widely used to analyse the initial stages of microphase separation for block copolymers and their mixtures.

2. Experimental evidence for TDGL kinetics in reactive processing of block copolymers

Both in situ and post mortem studies have been carried out on the formation and properties of poly(urea-co-isocyanurate), PUrI. In the former case [14], structure development was monitored using time-resolved synchotron SAXS. Micro-RIM apparatus was used to meter and

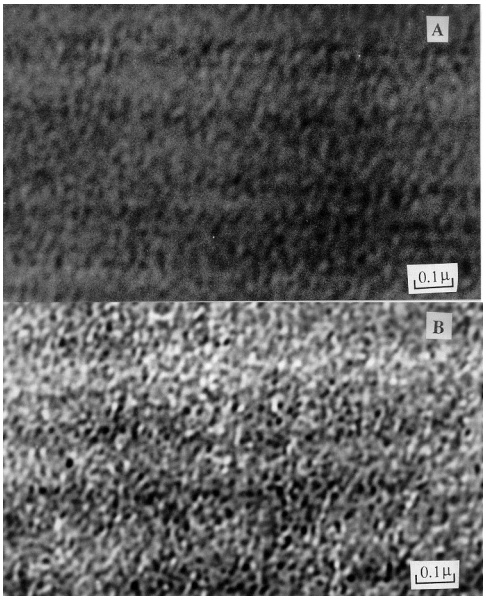

Fig. 2. TEM micrographs of a poly(ether-isocyanurate) with a volume fraction of polyether of 0.33. The contrast is due to variation in mass–density between the microphases and is enhanced by a slight underfocus. Micrograph A is for an as-moulded material and micrograph B for a material annealed for 1 h at 150°C [15].

mix the two reactants (methylene diphenyl isocyanate, MDI, and polyoxypropylene, POP, diamine), and to inject the reactant mixture into a mould-cell positioned in the optical bench assembly of the synchotron beamline. A typical scattering pattern from a copolymerisation carried out at 90°C is shown in Fig. 1(a) in which the microphase-separated structure is characterised by the development of a maximum in the scattering profile at $q^* \approx 0.065$ Å^{-1}. The inter-domain spacing (d) of this structure was calculated from the scattering maximum to give a value of $d \approx 97$ Å which agrees well with post-moulding values of d determined via static SAXS and TEM measurements on this system [15]. PUrI formation was studied at different temperatures in the range 70–135°C, and values of $I(q^*, t)$ were determined from SAXS data as a function of reaction time as shown in Fig. 1(b). At each temperature $I(q^*, t)$ versus t is characterised by an induction period (negligible growth), a period of rapid growth (microphase separation) and a plateau region (growth arrest). The onset times for microphase separation decrease with increasing temperature following an Arrhenius rate dependence, indicating that the microphase separation transition occurs at the same degree of isocyanate conversion, independent of temperature. Straight lines fit the growth regime on a semi-logarithmic plot, indicative of spinodal decomposition as predicted by the linearised theory of Cahn and Hilliard [26]. The initial 'wave' in the $I(q^*, t)$ data (at 110 and 70°C) before the straight line fit is due to the general rise in the background level following an upturn at a very low q due to scattering from gas bubbles. As expected for a block copolymer, the size scale of the growing structure is independent of temperature and the molecular connectivity between the polyether and polyisocyanurate phases restricts the inter-domain spacing to values $q^* R_g \approx 2$ as predicted by Leibler [16]. The radius of gyration R_g of combined hard block-soft block segments in the PUrI is not known, although values of R_g have been determined from SANS data for a POP pre-polymer of similar molar mass ($\approx$2000 g mol^{-1}) in a polyurethane block copolymer [17]. The radius of gyration $(R_g)_{POP}$ for POP chains was measured as 13.5 Å in the disordered (relaxed) state, and 16.0 Å in the ordered (stretched) state. Using these values for the PUrI, for which the volume fraction of POP is $\phi_{POP} = 0.43$ and R_g is approximated by $(R_g)_{POP}/\phi_{POP}$, gives values of $q^* R_g$ in the range 2.0–2.4. These values are typical of a block copolymer, that is the calculated values of d lie in the range $74 \leq d \leq 115$ Å and are in reasonable agreement with the experimental value of 97 Å determined from the SAXS data [14]. These studies lead to the somewhat surprising conclusion that a complex copolymerisation, producing ultimately a microphase-separated glassy polymer network, shows the Cahn–Hilliard kinetics of simple liquid–liquid phase separation.

Microphase separation is arrested prematurely by vitrification of the polyisocyanurate phase, and produces materials with non-equilibrium, bicontinuous morphologies. Some representative data from post mortem studies on the as-moulded and post-cured PUrI materials are shown in Fig. 2 [15]. The TEM micrographs show that high-temperature annealing improves the phase contrast of the microphase-separated structure, as confirmed by the increases in both the peak intensity $I(q^*)$ and the scattering power or invariant [15] in the static SAXS data. These data confirm the co-continuous morphologies (with length scales ~100 Å) of the post-cured PUrI materials, which may be classed as rubber-modified resins exhibiting two glass transition temperatures, one at −40°C associated with the polyether rubber phase, and the other at ~180°C associated with the crosslinked polyisocyanurate phase.

Both in situ scattering and post mortem TEM studies have been carried out on the formation and properties of PU foam. Flexible polyurethane foam is formed by simultaneous reactions of a diisocyanate with a polyether polyol and with water. The combination of these two exothermic reactions leads to the formation of a segmented block copoly(urethane-urea) [18–20]. During copolymer formation and as viscosity increases, foaming occurs by the co-generation of carbon dioxide gas evolved from the water–isocyanate reaction. Morphological development of the copolymer during foam formation is complex [18] and is caused by the increase in χN moving the system through a phase boundary. As copolymerisation proceeds, the core of the rising foam bun becomes self-insulated by the surrounding polymerising mixture creating, in effect, a quasi-adiabatic temperature environment. In situ SAXS experiments during foam formation, employing a forced-adiabatic SAXS sampling cell positioned in the optical bench assembly of a synchrotron beam line, have been reported by Elwell et al.

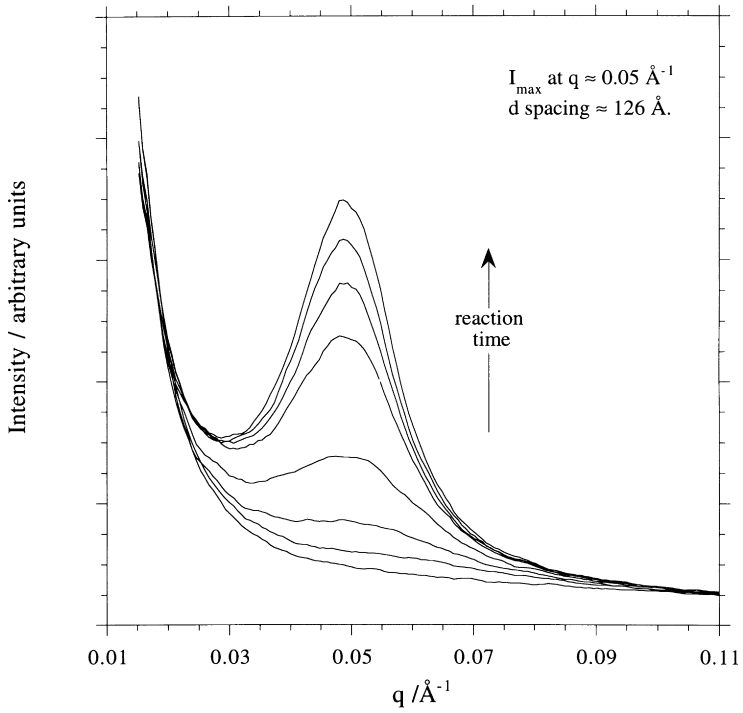

Fig. 3. Time resolved SAXS patterns obtained during the polymerisation of a poly(ether-urea) foam with a volume fraction of polyether of 0.71. SAXS intensity, $I(q)$ versus scattering vector, q, at increasing times during an adiabatic reaction with $\Delta T \sim 140$°C [7,19].

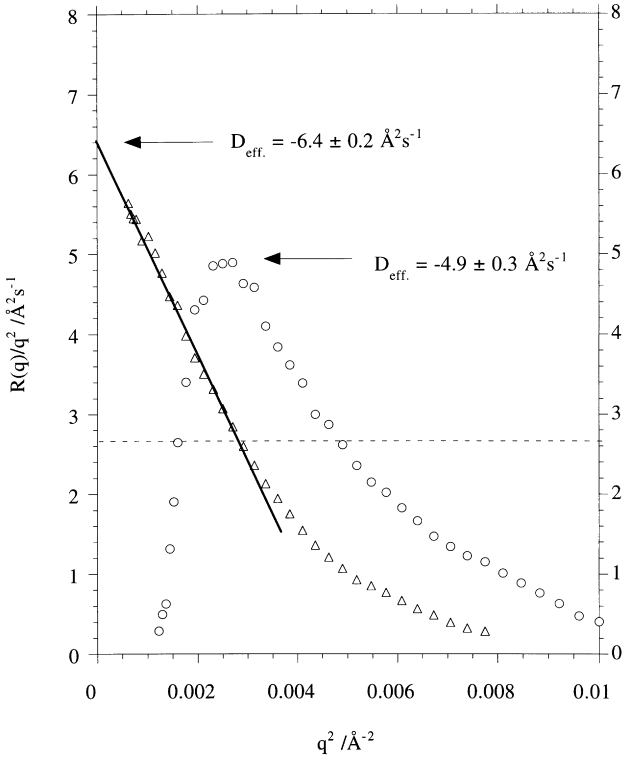

Fig. 4. TDGL analysis (plot of $R(q)/q^2$ versus q^2) of the SAXS data obtained during the adiabatic polymerisation of lightly crosslinked (□) and linear (△) poly(ether-urea) [19].

[7]. Representative time-resolved SAXS data that have been collected during foam formation (at 2 s intervals) are presented in Fig. 3 for an MDI based PU foam [7]. The patterns illustrate that in the early stage of the reaction, there is a homogeneous liquid present. At the microphase separation transition there is the first appearance of a scattering maxima and the intensity of this peak continuously increases. Eventually, the growth slows down and the peak intensity becomes approximately constant. This is after the microphase separation is arrested by vitrification of the phase that is richer in hard segment. The maximum in $I(q)$ suggests the presence of structure with periodic electron density within the sample. For this PU system the maximum in $I(q)$ occurs at $q \sim 0.06$ Å^{-1} giving an interdomain spacing of 105 Å. One of the conclusions of this work [7,19,20] was that the d spacing did not change during the structuring process for many PU systems.

The material that starts to order is a combination of homopolymer, block copolymers and monomers and is discussed in terms of a mixture. The final structured material is predominantly a block copolymer; and thus the data was also analysed in terms of the TDGL theory for microphase separation. The scattering patterns taken, as a function of time, during reaction have been analysed to obtain the composition amplification rate at discreet wave vectors, $R(q)$ defined by $I(q) = I_0(q) \exp[2R(q)t]$. For microphase separation via spinodal decomposition (TDGL), a plot of $R(q)/q^2$ versus q^2 (a measure of the thermodynamic driving force for phase separation) should exhibit a maximum at a finite value of q [21–25]. Fig. 4

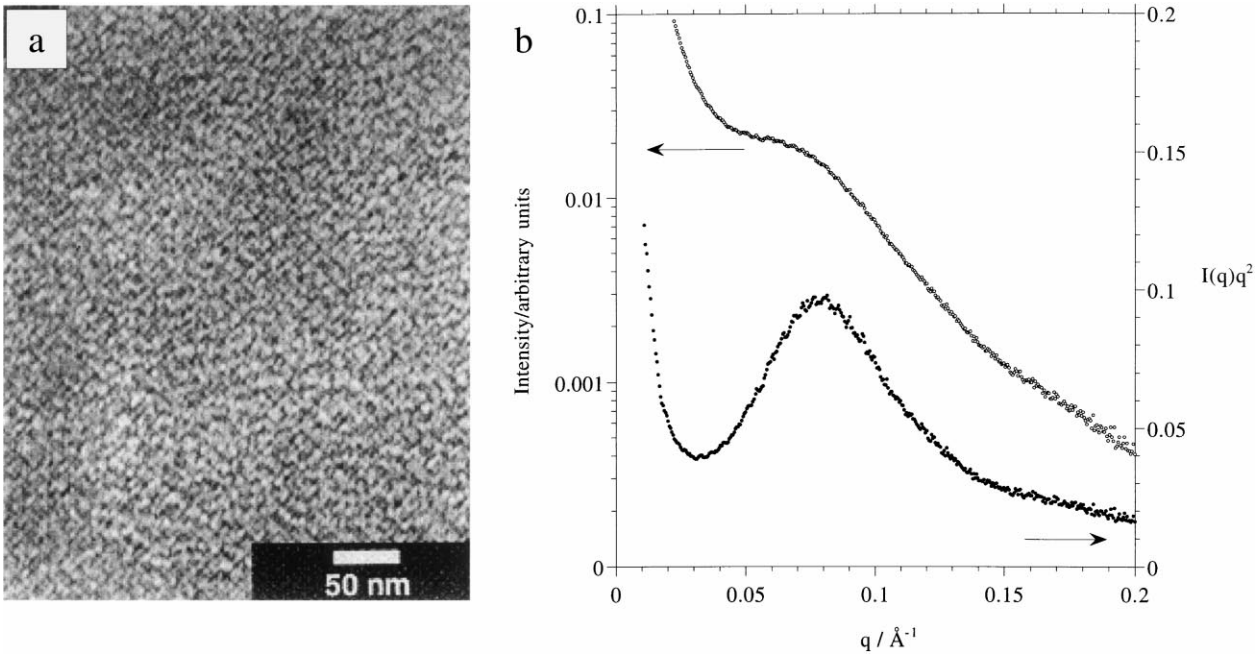

Fig. 5. (a) TEM of TDI based poly(ether-urea) foam with a volume fraction of polyether of 0.73. (b) SAXS corresponding to the foams in (a) [29].

shows representative plots of $R(q)/q^2$ versus q^2 for a lightly crosslinked PU system and a linear PU system based on a hydroxy functional three-arm star and a single arm, respectively. The crosslinked PU shows a peak in the curve [22] of $R(q)/q^2$ versus q^2 and the effective diffusion coefficient, D_{eff}, was calculated to be -4.9 ± 0.3 Å^2 s^{-1}. The negative diffusion coefficients indicate diffusion against the composition gradient (i.e. from a region of low concentration to a region of high concentration) as found in spinodal decomposition of a mixture [26]. For the linear system no maximum in $R(q)/q^2$ versus q^2 is observed. The linear behaviour at low values of q can be extrapolated to $q^2 = 0$; allowing the effective diffusion coefficient, D_{eff}, to be calculated as -6.4 ± 0.2 Å^2 s^{-1} [19,20].

Polyurethane phase separation has been studied extensively by post-mortem techniques and the combination of TEM and SAXS has been used to probe the morphology. Cooper and Li [27] claimed lamellar and cylindrical morphologies for a series of PU elastomers with semi-crystalline hard segments from TEM, whist SAXS showed single broad peaks with $d \sim 100$ Å. A SAXS and TEM study of flexible PU foam materials [28] showed a SAXS peak at $d \sim 100$ Å with a "fuzzy" morphology at this length scale with large precipitated "urea-balls" of $\approx$0.1 μm. Neff et al. [29] and Dounis and Wilkes [30] have used SAXS and TEM to investigate the morphology of a wide range of lightly crosslinked PU foams based on toluene diisocyanate, TDI. Fig. 5 presents TEM micrographs and SAXS patterns for poly(ether-urea) foam with a volume fraction of polyether of 0.73. There is strong evidence from these studies to support a microphase-separated morphology even though it is difficult to define in terms of the classical block copolymer structures. The micrographs show a two-phase structure with a strong resemblance to the Cahn–Hilliard random co-continuous structure [26]. The SAXS patterns show only a single broad peak similar to those in Fig. 3 obtained during polymerisation. The TEM and SAXS patterns correspond to a melt structure that has been trapped by vitrification. The SAXS patterns develop in a self-similar manner during reaction and by corollary it is highly likely that the final TEM micrographs are representative of the PU structure during polymerisation and the morphology is a relic of the arrested phase separation.

3. Cell dynamics simulations

In the CDS method, the time evolution of the order parameter ψ (given by Eq. (1) for di-block copolymers) is followed:

$$\frac{\partial \psi(\mathbf{r},t)}{\delta t} = M\nabla^2\left(\frac{\partial F}{\partial \psi}\right) + \eta(\mathbf{r},t) \tag{2}$$

Here M is a mobility coefficient, which is assumed to be constant and $\eta(r,t)$ is the random thermal noise term, which for a system in equilibrium at temperature T satisfies the fluctuation–dissipation theorem. The free energy functional is taken to be of a Landau–Ginzburg form. In the notation of

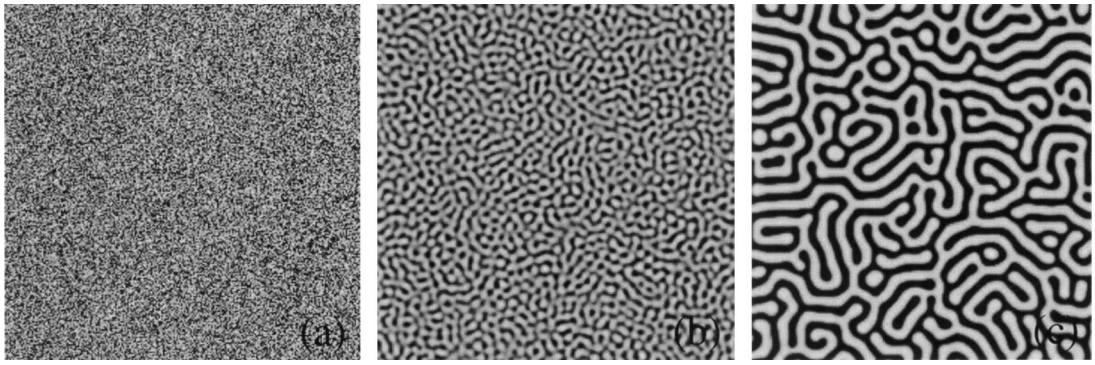

Fig. 6. Time series from CDS showing: (a) initial; (b) intermediate; and (c) late morphologies corresponding to 1, 100 and the final time-invariant (1000) iterations of the cell dynamics code.

Qi and Wang [11,12] it is given by

$$F[\psi(\mathbf{r})] = \int \mathrm{d}\mathbf{r}\left\{\psi(\mathbf{r})\left[-\frac{\tau}{2}+\frac{a}{2}(1-2f)^2-\frac{b}{2}\nabla^2\right]\psi(\mathbf{r}) + \frac{v}{3}(1-2f)\psi(\mathbf{r})^3+\frac{u}{4}\psi(\mathbf{r})^4\right\} + \frac{c}{2}\int \mathrm{d}\mathbf{r}_1\int \mathrm{d}\mathbf{r}_2 G(\mathbf{r}_1-\mathbf{r}_2)\psi(\mathbf{r}_1)\psi(\mathbf{r}_2) \quad (3)$$

where τ is related to the ordering temperature, f the volume fraction of one block and the coefficients a, b, c, u and v can be computed by evaluating the vertex functions computed by Leibler [16]. The long-range interaction arises from the connectivity between blocks and satisfies $\nabla^2 G(\mathbf{r}_1-\mathbf{r}_2) = -\delta(\mathbf{r}_1-\mathbf{r}_2)$. A large class of physical systems with competing short-range and long-range interactions can be described by Eqs. (2) and (3). Eq. (2) is not limited to systems with conserved order parameters such as block copolymer melts. For block copolymers, it is applicable in the weak segregation limit because a single wave number dominates during structure formation in this regime.

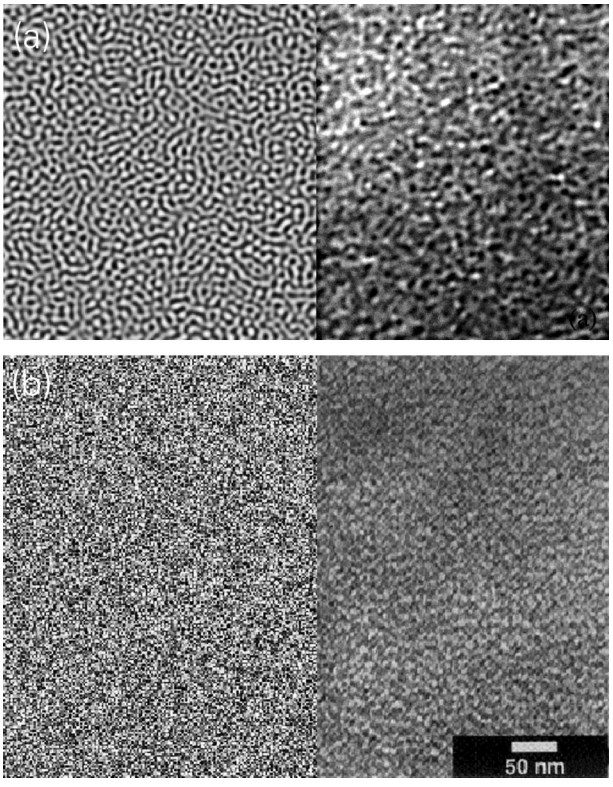

Fig. 7. Comparison of the appropriately scaled and thresholded CDS simulation (left) with the TEM micrographs (right) of (a) a copolyisocyanurate urea and (b) a polyurethane foam. In each case the CDS image at a given iteration was chosen for comparison as the qualitative "best match".

We have performed cell dynamics simulation using the deterministic equations obtained by Puri and Oono [10]. The discretized order parameter after step $t+1$ is given by

$$\psi(t+1,n) = f(\psi(t,n)) \quad (4)$$

where $f(x)$ is represented by $A\tanh x$. This corresponds to the functional form for the interfacial profile in the evolved structure. The time evolution of the order parameter follows

$$\psi(t+1,n) = f(\psi(t,n)) + D[\langle\langle\psi(t,n)\rangle\rangle - \psi(t,n)] \quad (5)$$

where D is a positive constant proportional to the phenomenological diffusion constant. The quantity $\langle\langle * \rangle\rangle$ represents a spatial average, which for a two-dimensional square lattice is written [10]

$$\langle\langle\psi(t,n)\rangle\rangle = \frac{1}{6}\sum_{i\in\{\mathrm{nn}\}}\psi_i + \frac{1}{12}\sum_{i\in\{\mathrm{nnn}\}}\psi_i \quad (6)$$

where nn denotes nearest neighbour cells and nnn next nearest neighbour cells.

Simulations were performed on a 256×256 lattice using FORTRAN code running on a SparcStation 20. The values $A=1.3$, $D=0.5$ were used [10]. Starting from an initial configuration in which the order parameter takes a random value from a uniform distribution with amplitudes in the range $A_\mathrm{i}=-0.05$ to 0.05 (corresponding to weak fluctuations in the disordered state), these values of A and D are associated with a quench into a weakly ordered heterogeneous state [10]. An image corresponding to the starting configurations is shown in Fig. 6(a). Images were also

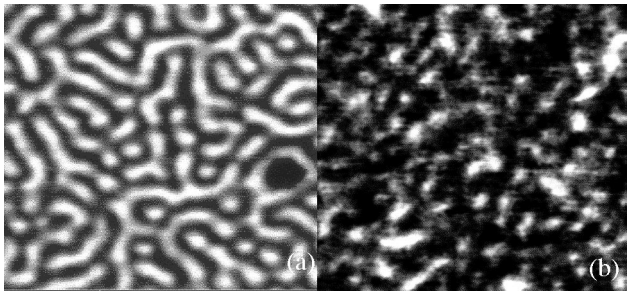

Fig. 8. Tapping mode AFM topographs of (a) a SEBS triblock copolymer which is 0.7 polyolefin and 0.3 polystyrene and (b) Pelethane polyurethane which is approximately 0.8 polyether. The scales for each image are different (because of the block lengths of the polymers) and have been chosen so the images have similar characteristic lengths [31].

obtained during the evolution of the microphase-separated structure. Patterns were obtained after 100 iterations, Fig. 6(b), corresponding to an early stage of structure development, and after 1000 iterations, giving a fully developed (time invariant) structure, Fig. 6(c).

The cell dynamics simulations are able to capture the features observed in the TEM images for PU block copolymers. In particular, at the intermediate stage of structure development, CDS shows a microphase-separated morphology with an irregular co-continuous structure without long-range order (Fig. 6(b)). This strongly resembles the TEM images in Figs. 2(b) and 5(a). In contrast, the morphology achieved at equilibrium in the simulations is a highly developed lamellar structure, with random orientation of lamellae (Fig. 6(c)). This type of morphology is not observed in the TEM of PU. Fig. 7 presents a comparison of the appropriately scaled and thresholded CDS simulation with the TEM micrographs of a copolyisocyanurate urea and a polyurethane foam. In each case the CDS image at a given iteration was chosen for comparison as the qualitative "best match", this process is necessarily arbitrary. However, the observations are consistent with a scenario previously suggested for morphology development in polyurethanes [4–7,14,15,17,19,20], that is microphase separation occurs into a weakly ordered structure with no long-range positional or orientational order. Further evolution into a structure with well-segregated domains is prevented by vitrification (or crosslinking) of the hard segments. Thus microphase separation is arrested in the early stages and the CDS method provides a powerful means of simulating this process, which has yet to be modelled by analytical theories.

Atomic force microscopy has recently been used to study block copolymer morphology and provides a good illustration of the features of PU with quenched structures that differ from those of block copolymers with equilibrium structures [31]. The topographical image in Fig. 8(a) shows quite clearly how a polystyrene–poly(ethylene-ran-butylene)–polystyrene tri-block copolymer, which has a narrow molecular weight distribution blocks and a simple chain structure, can arrive at an equilibrium morphology which is strikingly similar to the time invariant result of the CDS simulation in Fig. 6(c). In this case the microphase separation process has been completed prior to vitrification. The topographical image of a polyurethane in Fig. 8(b) has an uncanny resemblance to the intermediate result of the CDS simulation in Fig. 6(b) and in this case the phase separation was arrested by vitrification.

Scattering studies of the phase separation kinetics in block copolymers are not common and there have been few studies [22,32–34] which claim to access the early stages of microphase separation. The molecular connectivity in block copolymers restricts the spatial extent of the concentration fluctuations to dimensions of approximately twice the radius of gyration (R_g) of the entire block chain ($\approx$200 Å). The scattering data are analysed by a generalised time-dependent Ginzburg–Landau model of microphase separation kinetics proposed by Hashimoto and employed by Connell and co-workers [22]. The CDS scheme used here is closely related to that used by Hashimoto[25], although is should be noted that there is a long-range order term in Eq. (3). It is reasonable to assume a model that predicts the evolution of the scattering patterns and predicts the final morphology also makes a good job of predicting the development of the real-space structure. It should be noted that Fig. 6(b) and (c) shows considerable coarsening, i.e. an increase in pattern size which corresponds to s decrease in q^*. This behaviour is not seen in the scattering data of Figs. 2–4 and illustrates that the phase separation process is limited to the early stages, that is constant q^*.

The interpretation of morphology in the multi-block polymers discussed above is further complicated by the fact that they are often highly branched or even cross-linked. The structure observed in multi-blocks made by direct polycondensation indicates that long-range order is not attainable even though this would be the equilibrium state. Studies of di-block copolymers show that the ordering process is two stage with an initial formation of the morphological units (spheres, rods, lamellae) followed by a co-operative reorganisation into a structure with long-range order [32–34]. It could be that the first process is all that occurs in multi-blocks and the morphology gets stuck at this stage as the co-operativity required to get long-range order, from chains which may reside in up to ten domains, is not available. The combination of block length polydispersity and no long-range order would certainly account for the broad scattering peaks obtained from SAXS and SANS observed for multi-blocks made by direct polycondensation. In agreement with these observations, the mean field theory of Fredrickson et al. [35] predicts that the long-range order is suppressed in microphase-separated multi-block copolymers due to a broad distribution of monomer sequence lengths. An alternative explanation is that the structure observed in multi-blocks are composition fluctuations pinned by vitrification of the glassy microphase. This is almost certainly the case for block copolymers where the glassy phase has a high T_g [3]. Evidence for

this mechanism is also provided by the constant q^* during morphology development.

Multi-block copolymers have been made by anionic polymerisation so that the effect of block number could be systematically studied. In an elegant TEM and SAXS study Smith et al. [36] and Spontak [37] showed that even for styrene–isoprene $(SI)_n$ multi-block polymers made by anionic polymerisation long-range order was reduced for $n = 4$. As n increases the lamella are observed to be thinner and the long-range order decreases. This suggests that it is the multi-block nature of the PUs that leads to the absence of long-range order.

4. Summary and conclusions

We have compared the experimental observations of the kinetics of microphase separation during the reactive processing of multi-block copolymers and their final morphology with a cell dynamics simulation. The TDGL model is widely used to analyse the initial stages of microphase separation for linear di-block and crosslinked multi-block copolymers. A TGDL based cell-dynamics model gives indications of the morphology for reactively processed multi-block copolymers, which do not have an equilibrium morphology, and anionic tri-block copolymers, which do have an equilibrium morphology.

The purpose of this paper was to compare experimental and simulation results for structure development during a copolymerisation reaction. The model used did not incorporate any reactive aspects, and this represents a serious flaw in our argument. However, the simulation had the same mathematics as that found in the scattering studies of structure development. The initiation of structure formation is caused by the polymerisation driving the system across a phase boundary, the kinetic limitation to structure formation is vitrification of one of the (micro)phases. It would appear that the structuring mechanism is somewhat insensitive to the reaction (once phase separation has been induced) and this is borne out by the comparisons made here. It is our hypothesis that the similarity between the structures is not superficial and that they correspond to the same dynamical stage. Future work will incorporate the effects of chemical reaction into the CDS model to test this hypothesis. Read [38] has described a mean field theory for phase separation during polycondensation, the theory gives structure factors that change, qualitatively, like the scattering patterns in Fig. 3 as a function of conversion. The theory allows spinodals to be calculated but predictions of the dynamics have not yet been published.

The conclusion of this study is that the multi-block systems show pinning of the microstructure at early stages of microphase separation in contrast to the equilibrium structures formed by di- and tri-block copolymers.

Acknowledgements

Our (MJE, JLS, ANW and AJR) experimental work on isocyanate-based materials reported here has been generously supported by the EPSRC (GR/J24713), The Dow Chemical Company and Kobe Steel Europe. The simulations were supported by a EPSRC(GR/M08523) grant to IWH. Dr Sauer generously provided the images used to prepare Fig. 8.

References

[1] Hamley IW. The physics of block copolymers. Oxford: Oxford University Press, 1998.
[2] Legge NR, Holden G, Schroeder HE. Themoplastic elastomers. Munich: Hanser, 1993.
[3] Macosko CW. RIM: fundamentals of reaction injection molding. Munich: Hanser, 1988.
[4] Ryan AJ. Polymer 1990;31:707.
[5] Ryan AJ, Stanford JL, Still RH. Plast Rubb Proc Appl 1990;13: 99.
[6] Stanford JL, Elwell MJ, Ryan AJ. Processing of polymers. In: Cahn RW, Haasen P, Kramer EJ, editors. Materials science and technology: a comprehensive treatment, vol. 18. Weiheim: VCH, 1998. p. 465 chap. 9.
[7] Elwell MJA, Ryan AJ, Mortimer S. Macromolecules 1994;27: 5428.
[8] Bahiana M, Oono Y. Phys Rev A 1990;41:6763.
[9] Chakrabarti A, Toral R, Gunton JD. Phys Rev A 1991;44:6503.
[10] Puri S, Oono Y. Phys Rev A 1988;38:1542.
[11] Qi S, Wang ZG. Phys Rev Lett 1996;76:1679.
[12] Qi S, Wang ZG. Phys Rev E 1997;55:1682.
[13] Shiwa Y, Taneike T, Yokojima Y. Phys Rev Lett 1996;77:4378.
[14] Wilkinson AN, Naylor S, Elwell MJ, Draper P, Komanschek BU, Stanford JL, Ryan AJ. Polymer 1996;37:2021.
[15] Ryan AJ, Stanford JL, Toa XQ. Polymer 1993;34:4020.
[16] Leibler L. Macromolecules 1980;13:1602.
[17] Naylor S, Terrill NJ, Yu GE, Tanodekaew S, Bras W, King SM, Booth C, Ryan AJ. Polym Int 1997;44:371.
[18] Artavia LD, Macosko CW. J Cell Plast 1990;26:490.
[19] Elwell MJ, Ryan AJ, Grünbauer HJM, Van Lieshout HC, Lidy W. Plast Rubb Proc Appl 1995;23:265.
[20] Elwell MJ, Ryan AJ, Grünbauer HJM, Van Lieshout HC. Macromolecules 1996;29:2960.
[21] Olabisi O, Robeson LM, Shaw MT. Polymer–polymer miscibility. New York: Academic, 1977.
[22] Connell JG, Richards RW, Rennie AR. Polymer 1991;32:2033.
[23] Bates FS, Wiltzius P. J Chem Phys 1989;91:3258.
[24] Binder K. Phase transformations in materials. In: Cahn RW, Haasen P, Kramer EJ, editors. Materials science and technology: a comprehensive treatment, vol. 5. Weinheim: VCH, 1991. p. 405 chap. 7.
[25] Hashimoto T. Macromolecules 1987;20:465.
[26] Cahn JW, Hilliard J. J Chem Phys 1958;28:258.
[27] Cooper SL, Li C. Polymer 1990;31:3.
[28] Armistead JP, Turner RB, Wilkes GL. J Appl Polym Sci 1988;35:601.
[29] Neff R, Adedeji A, Macosko CW, Ryan AJ. J Polym Sci Polym Phys Ed 1998;36:573.
[30] Dounis D, Wilkes GL. J Appl Polym Sci 1997;65:525.
[31] McLean RS, Sauer BB. Macromolecules 1998;30:8314.
[32] Singh MA, Harkless CR, Nagler SE, Shannon RF, Ghosh SS. Phys Rev B 1993;47:8425.
[33] Gupta JA, Singh MA, Salomons GJ, Foran WA, Capel MS. Macromolecules 1998;31:3109.
[34] Stuhn B, Vilesov A, Zachmann HG. Macromolecules 1994;27: 3560.
[35] Fredrickson GH, Milner ST, Leibler L. Macromolecules 1992;25:6341.
[36] Smith SD, Spontak RJ, Satowski MM, Ashraf A, Heape AK, Lin JS. Polymer 1994;35:4527.
[37] Spontak RJ, Smith SD, Ashraf A. Macromolecules 1993;26:5118.
[38] Read DJ. Macromolecules 1998;31:899.